DINAME 2023 - Proceedings of the XIX International Symposium on Dynamic Problems of Mechanics,
A.S. De Paula, A.T. Fabro and M.R. Machado (Editors), ABCM.
Pirenópolis, Go, Brazil, February 26th to March 3rd, 2023

An experimental investigation of the fluid-structure coupling in horizontal pipes conveying two-phase flows

DA das Neves[1], SC Vieira[2,3], AT Fabro[1], JR Cenzi[3], DM Iceri[4] and MS Castro[2,4]

[1] Department of Mechanical Engineering, University of Brasilia, Brasília-DF, Brazil

[2] PETROBRAS, Santos-SP, Brazil

[3] School of Mechanical Engineering, University of Campinas, Campinas-SP, Brazil

[4] Center for Petroleum Studies, University of Campinas, Campinas-SP, Brazil

Abstract:
Studies involving two-phase flow are extremely important for the petrochemical industry because the way in which the phases are distributed dictates the behavior of the gradient of pressure and quantities such as the heat transfer coefficients of the mixture, in addition to being relevant in flow assurance problems. Therefore, this work studies the fluid-structure coupling in two-phase flows in horizontal pipes through the analysis of pressure and acceleration signatures. The results indicate a region of fluid-structure coupling from 2400 Hz to 3400 Hz, called coincidence frequency. Where the circumferential mode frequency of pipe is very close the resonance frequency of the bubble, in the liquid piston for intermittent patterns.

Keywords: fluid-structure coupling, two-phase flow, cylindrical shells

INTRODUCTION

The intermittent flow pattern is problematic for practical operations due to changes of moment and pressure fluctuations causing the pipe resonant oscillations (Hara, 1977, Miwa, 2015). Then, fluid flow in pipes is a typical Fluid Structure Interaction (FSI) phenomenon, in which the flow excites the pipe and consequently it is deformed, named one-way coupling. On other hand, the two-way coupling consider that excitation of the flow causes deformations in the walls pipe and it also excites the flow (Mohmmed, 2020). Nevertheless, due to its complexity, few studies have investigated two-way coupling, so the most assume the one-way coupling to analyze the dynamic response analytically and computationally. Figure 1 presents the physical model for slug flow. It consists of alternating repetitive arrangements, called unit cells with length L_U along the pipe with a characteristic frequency. These cells are composed of liquid pistons aerated by small dispersed bubbles of length L_S followed by a Taylor bubble of length L_F. In addition, there is a turbulence zone behind the Taylor bubble passage defined as L_M.

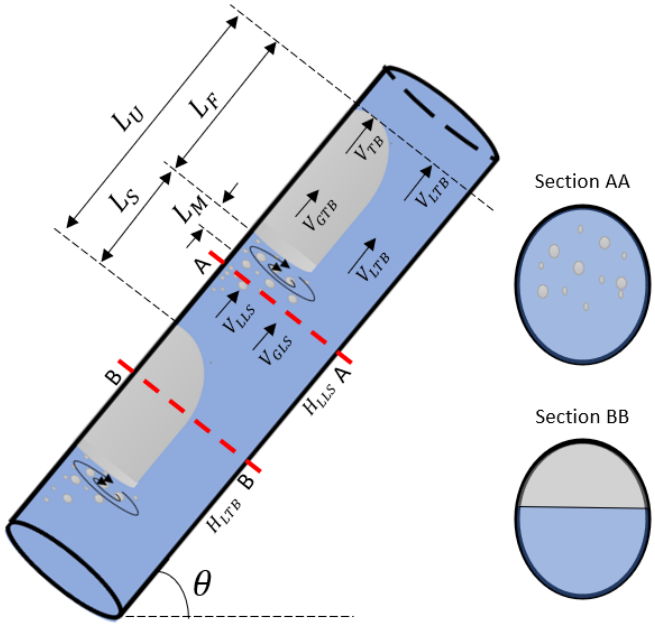

Figure 1 – Slug flow characteristics (adapted) (Shoham, 2006).

Dispersed phase bubbles present in the liquid piston in the intermittent pattern are deformable and compressible, in two-pahse gas-liquid flows. More significantly, the study of this phenomenon involves understanding the processes of coalescence break up as well as any phase changes occurring. The coalescence process is responsible for the evolution of fluid bubbles sizes, together with break up and mass transfer due to particle growth. Liao (2009) pointed out a variety of mechanisms for breaking the bubble that include turbulent fluctuation and collision or turbulent shearing, viscous shear force, interfacial instability and shearing-off process. Furthermore, an important mean diameter for these bubbles is called the Hinze diameter is based on the concept of turbulent forces overcoming surface tension forces, dispersing the gas phase into small bubbles in the continuous phase. According to Zhao (2021), the bubbles larger than Hinze diameter ($d_i > d_H$), called super-Hinze region, tend to follow a $-10/3$ power scaling with respect to the major length, in addition the surface tension can hold the bubble shape against the shear forces in a turbulent flow. However, for diameter smaller than the diameter of Hinze ($d_i < d_H$), called Hinze-scale, the surface tension can hold the bubble shape against the shear forces in a turbulent flow.

Another important point is that the bubbles are deformable and compressible, which allows the movement of contraction and expansion. When a bubble is placed in an acoustic field with wavelength much larger than the bubble diameter it undergoes radial oscillations. Depending on the intensity of the driving force, the bubble may oscillate linearly around its equilibrium radius, oscillate nonlinearly or even collapse. For small amplitudes, the bubble oscillates linearly. For increasing amplitude, the bubble may oscillates nonlinearly and until it collapses. For the linear case, the bubble will compress while the pressure is positive and expand when it is negative. So, the radial oscillation is inversely proportional to the pressure of the continuous phase, and this works as a harmonic oscillator. Therefore, there is a periodic variation of the small amplitude radius with a characteristic frequency during the time the bubble is under the pressure field (Brennen, 2005). Therefore, the Fluid-structure coupling between a structural frequency of the duct and the resonant frequency of the bubbles is investigated through vibration and pressure signals acquired from a two-phase experimental test in a horizontal duct.

Fluid-structure coupling

An important behavior is observed when an acoustic frequency is equal or close to the structural mode, called coincidence phenomenon. It is related by an increase in the vibrational response in the this frequency. This phenomenon is usually observed at frequencies close to the cut-off frequencies of the cylindrical shells due to the circumferentially combined character of the structural and acoustic waves of the wavenumber. According to Fahy e Gardonio (2015), this phenomenon is important to determine the coupling between this two domains. But there are few literature studies on single-phase and two-phase internal flow applications.

The vibroacoustic behavior of pipe conveying two-phase flow has not been extensively addressed, although the sound field also excites the structure generating vibrations. Fuller and Fahy (1982) investigated the dynamic behavior of thin-walled cylindrical elastic shells filled with fluid, where reported that energy in specific modes can be transferred between the fluid and the structure depending on the excitation frequency and the modal characteristics of the coupled system. Norton e Bull (1984) investigated the phenomenon of acoustic radiation in turbulent internal flow, where identified the coupling of structural and acoustic modes close to the cut-off frequency.

The problem involves the coupling of structural and fluid, so the main difficulties include the coupling of the wave propagation equation to the pipe wall and fluid. Kirby (2019) observed the phenomenon of energy transfer between the fluid and the structure using a semi-analytic method to couple the elastodynamic wave equation for the pipe wall to convected wave equation for sound propagation in a uniform fluid flow. Figure 2 presents is possible to observe the fundamental fluid type mode comes close to a structural type mode, but avoids crossing and, therefore, energy is transferred from the fluid to the structure. In addition, the author concluded that the mean flow significantly changes the radiation characteristics of acoustic pipes, with a directly proportional relation.

Resonant frequency of the bubbles

As previously discussed, a bubble in a liquid can be considered an oscillator due to the elastic behavior of the non-condensable gas that the bubble contains and the inertia of the liquid. Therefore, a natural frequency is associated with bubble oscillatory dynamics in a liquid that can be derived from the Rayleigh-Plesset equation in the absence of thermal effects and liquid compressibility effects. Thus, the natural frequency of oscillation of the bubbles f_r, also named Rayleigh-Plesset frequency, is represented by,

$$f_r = \frac{1}{2\pi}\sqrt{\frac{1}{\rho_L R_0^2}\left(3K(\overline{p_\infty} - p_V) + 2(3K-1)\frac{\sigma}{R_0}\right)}, \tag{1}$$

where $\overline{p_\infty}$ is mean pressure value, R_0 is the radius of the bubble, K is the polytropic coefficient, p_v the vapor pressure which depends only upon the temperature, and ρ_L is the density of liquid and σ s the surface tension.

The bubble diameter considered is the Hinze diameter witch is is based on the concept of turbulent forces overcoming

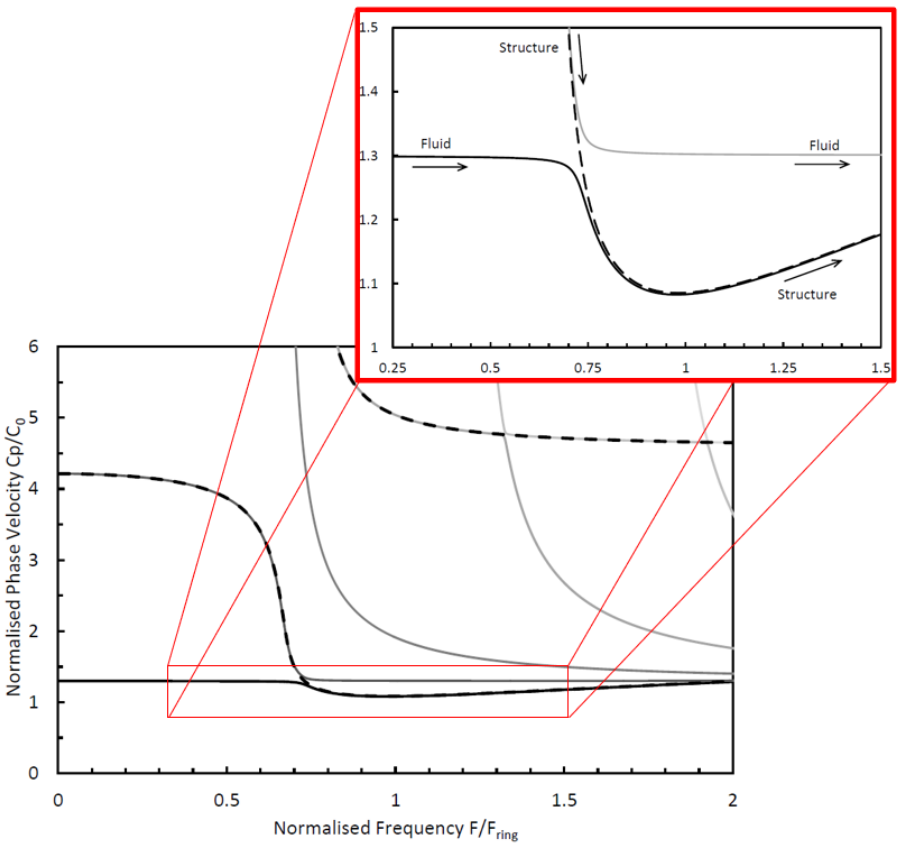

Figure 2 – Coupling between the fluid and the structure obtained by Kirby (2019) (adapted). Full black lines are coupled fluid type modes, dashed black lines are uncoupled structure modes and full gray lines are coupled higher order compressional modes.

surface tension forces, dispersing the gas phase into small bubbles in the continuous phase (Hinze, 1955), (Barnea, 1985) and (Calderbank, 1958). Thus, the expression for Hinze diameter is,

$$d_H = (0.75 + 4.15\sqrt{\alpha}) \left(\frac{\sigma}{\rho_L}\right)^{0.6} \left(\frac{2 f_M v_M}{d}\right)^{-0.4}, \tag{2}$$

where f_M is the mixture friction factor, v_M is the velocity of mixture, α is the void fraction and d is the diameter of pipe.

Cylindrical shells

The cylindrical shell is a structure limited by two curved surfaces, in which the distance between these surfaces is small in relation to the other dimensions, radius and length. The circumferential modes are related to the mechanical waves present in the structure and are different from the vibration modes associated to the natural frequencies of a finite length structure. The axial modes are flexural deformations along the axial direction (Fahy, 2015).

For low frequency, domain below the frequency of the ring is the zone dominated by the stiffness of the structure. In a "bending mode", $n = 1$, the cylindrical shell oscillates around the axial axis while radial displacements remain unchanged, in other words, the structure behaves like a beam corresponds to a rigid body mode. Therefore, in an empty cylindrical shell, the frequencies of the other circumferential modes are determined by the non-dimensional frequency parameter,

$$\Omega_n^2 = \left(\frac{h}{\sqrt{12}r}\right)^2 n^4 \left[1 - \frac{1}{2}\left(\frac{1}{1-\nu}\right)\left(\frac{4-\nu}{n^2} - \frac{2+\nu}{n^4}\right)\right]. \tag{3}$$

where $\Omega = \omega/\omega_1$, $\omega_1 = \sqrt{E/\rho r^2}$, E is modulus elasticity, ρ is the mass specific, ν is the coefficient of Poisson, r is the radius and h is the thickness of pipe. The ring frequency associated to the circumferential order $n = 0$ exhibits a resonance frequency higher than that for $n = 2$ due to the effect of curvature of the ring stiffener,sometimes the ring frequency can be higher than the $n = 3, \ldots, N$ frequencies.

EXPERIMENTAL SETUP

The horizontal line of two-phase liquid-gas flow was developed, consisting of a 15 meter section of NBR 5580 carbon steel pipe with 2" internal diameter and 4.5 mm of thickness. This pipe has modulus of elasticity, specific mass and Poisson of coefficient equal to 193.23 GPa, 7434.5 kg/m^3 and 0.30, respectively. The oil used in this test is of the Luchetti M600 mineral type with a viscosity of approximately 205 cP, at ambient temperature and an average density of 868 kg/m^3. The water has a viscosity of approximately 1 cP, at at ambient temperature, and an average density of 998 kg/m^3. At the end of the line, the viewing session was installed, where the camera was positioned to record the flow pattern and holdup. The distribution of sensors on the bench is shown in Figure 3, with four piezoelectric pressure sensors (P_{Z1},P_{Z2},P_{Z3} and P_{Z4}), two differential pressure sensors, two triaxial accelerometers (A_{T1} and A_{T2}) and four uniaxials accelerometers (A_{u1}, A_{u2}, A_{u3} and A_{u0}). The accelerometer A_{u0} was placed on the pipe support to analyse the boundary condition.

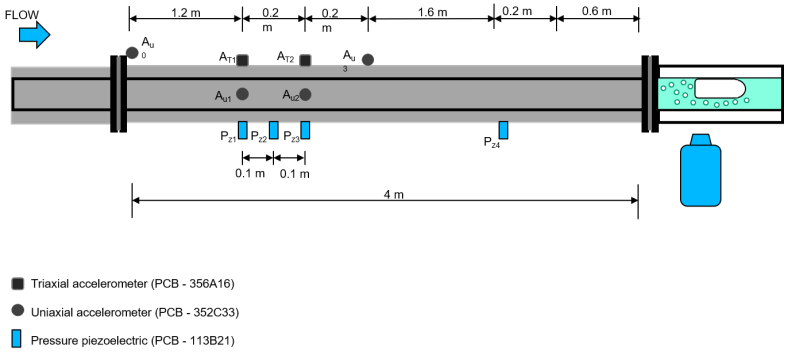

Figure 3 – Experimental setup and sensors configuration.

Figures 4 (a) and (b) presents the flow map for water-gas and oil-gas flow, respectively, using the model proposed by Barnea et al. (1980). The X-axis is the superficial velocity of gas (J_G) and Y-axis is the superficial velocity of Liquid (J_W and J_O). It was determined a set of 33 experimental points for water-gas flow and 34 for oil-gas flow. They are presented overlapping the flow map models, indicating the observed flow pattern by different symbols.

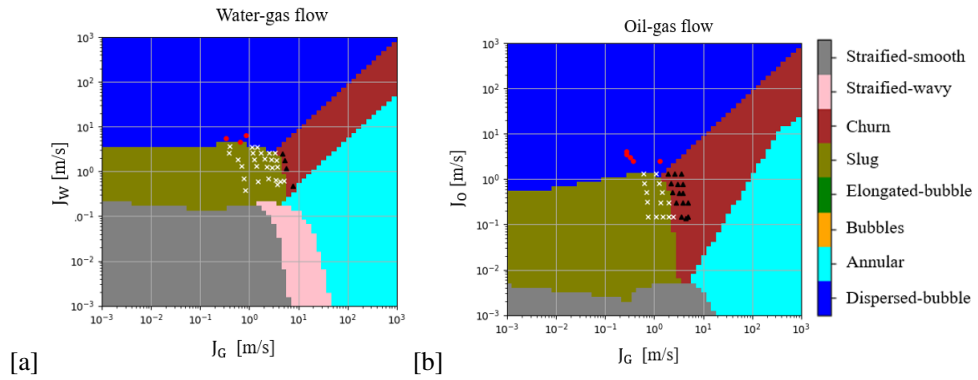

Figure 4 – Flow pattern map for water-gas (a) and oil-gas (b) flow according to the Barnea1980 model. Experimental points overlapping the map indicate the observed flow patterns as slug (×), churn (△) and dispersed-bubble (◯).

RESULTS

In this work, the natural frequencies (f_m) of the pipe was calculated by a simplified model of a Euler-Bernoulli beam convey fluid flow assuming simply supported boundaries conditions with torsional springs, which represent the bending stiffness of the pipe structural elements connected. This model can capture the low frequency behavior, these are related to local modes of the pipe and are greatly affected by the pipe geometry and boundary conditions, for example, the flange connections. Thus, the analytical values calculated were f_{m1} = 12.82 Hz, f_{m2} = 42.03 Hz, f_{m3} = 87.92 Hz, f_{m4} = 150.56 Hz. At higher frequencies, acoustic coincidence effects cause increased excitation of supersonic pipe modes, which increase wall vibrations and external noise radiation. The cut-off frequencies of the circumferential wave modes or cylindrical shells frequency (f_n) were calculated by Equation 3, the analytical values calculated were f_{n2} = 12.82 Hz, f_{n3} = 42.03 Hz.

Figure 5 presents the amplitude of the Discrete Fourier Transform (DFT) of the acceleration signal. The moving average technical with 50 samples was used for smoothing the curve of DFT. The first four natural frequencies $f_{m1,2,3,4}$ of the pipe convey the two-phase flow are identified in colored dots. Moreover, the shell frequencies $f_{n2,3}$ are marked with pink and gray dots respectively. It is observed that amplitude of the DFT is larger in first mode results, this can be caused by the presence of two-phase flow phenomena, for example, Taylor bubble with low frequencies affect the first mode peak frequency response. Furthermore, the frequency f_{n2} also has a very pronounced amplitude, it is in the zone of the fluid phenomenon that will be detailed in the next work.

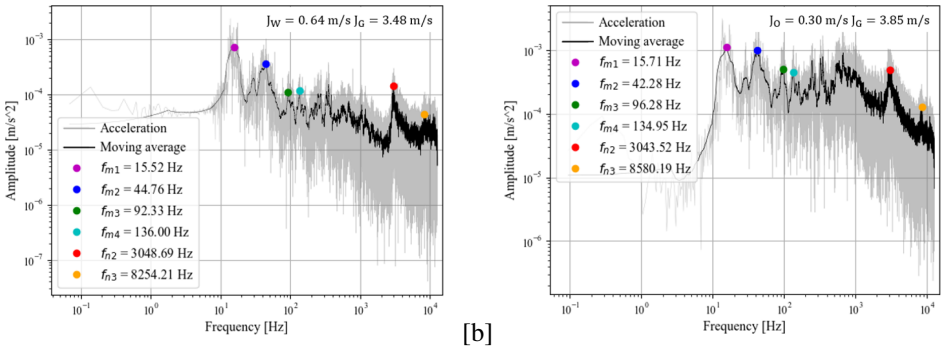

Figure 5 – The raw (gray line) and smoothed (black line) DFT of the acceleration signals for the 2" pipe for (a) water-gas and (b) oil-gas flow.

Figure 6, on the left, presents the time signal of pressure (P_{z1}) and acceleration signal envelope (A_{T1}) measured at the same position of pipe for intermittent pattern. A band-pass filter from 2400 Hz to 3400 Hz was applied in the acceleration signal, in the cylindrical shell frequency region (f_{n2}) and the envelope was obtained by applying the Hilbert transform. A low-pass filter with a cut-off frequency of 30 Hz was applied in the pressure signal, as discussed in Section **??** is the region where the main phenomena related to flow occur. On the right presents the DFT of the original acceleration signal (gray line) and a smoothing curve (black line), obtained using the moving average technique with 50 samples. The red dot indicates the cylindrical shell frequency and the blue line indicates the resonant frequency of the bubbles, calculated with the Hinze diameters. The superficial velocities of the phases (J_{sg} and J_{sl}) and the translational velocity (V_{TB}), slug frequency (f_s), resonance frequency (f_r) and flow pattern are also indicated. Thus, it is possible to observe that when f_r is close to fn_2, i.e., the blue line is near the red dot, the pressure and acceleration signals have an orderly behavior. The maximum amplitude of the pressure signal and the acceleration envelope signal are coincident, as shown in Figure 6 (c). According Carvalho (2020) the increase in the amplitude of the acceleration signal corresponds the transition region of piston liquid and Taylor bubble. Consequently, the maximum amplitude peaks of both signals indicate the passage of the Taylor bubble.

Figure 7 presents the pressure signal and acceleration envelope measured at the same point in the pipe, for oil-gas flow. As in the previous case, the acceleration signal was filtered in the cylindrical shell frequency region f_{n2} (2400 Hz-3400 Hz) and the pressure signal was filtered at 30 Hz. By doing so, it is possible to observe that the maximum amplitude of the pressure signal and the acceleration envelope signal are coincident for the cases (b) and (c). This behavior is also associated with increases the number of bubbles dispersed in the flow caused by the increase in the superficial velocity of the gas (Shoham, 2006).

In all cases, the Hinze diameter (d_H) was calculated by Equation 2 and the resonance frequency (f_r) was calculated using the Hinze diameter from Equation 1. These results indicate that a source of excitation for phenomenon of fluid-structure coupling, from 2400 Hz to 3400 Hz. Furthermore, in the following work, the flow parameters measured with the filtered signals in this region will be shown, as Taylor bubble velocity and slug frequency.

CONCLUSION

The results of the analysis of the structural vibration and pressure signals indicate an region of fluid-structure coupling from 2400 Hz to 3400 Hz, called coincidence frequency. Where the circumferential mode frequency of pipe is very close of resonance frequency of the bubble, in the liquid piston for intermittent patterns. As a consequence, it was possible to identify the Taylor bubble passage, to estimate the translational velocity and slug frequency in the coincidence frequency.

ACKNOWLEDGMENTS

We would like to acknowledge PETROBRAS (grant number 2017/00778-2) and ANP for the financial support of this research and the Artificial Lift and Flow Assurance Research Group (ALFA), to the *Experimental Laboratpry of*

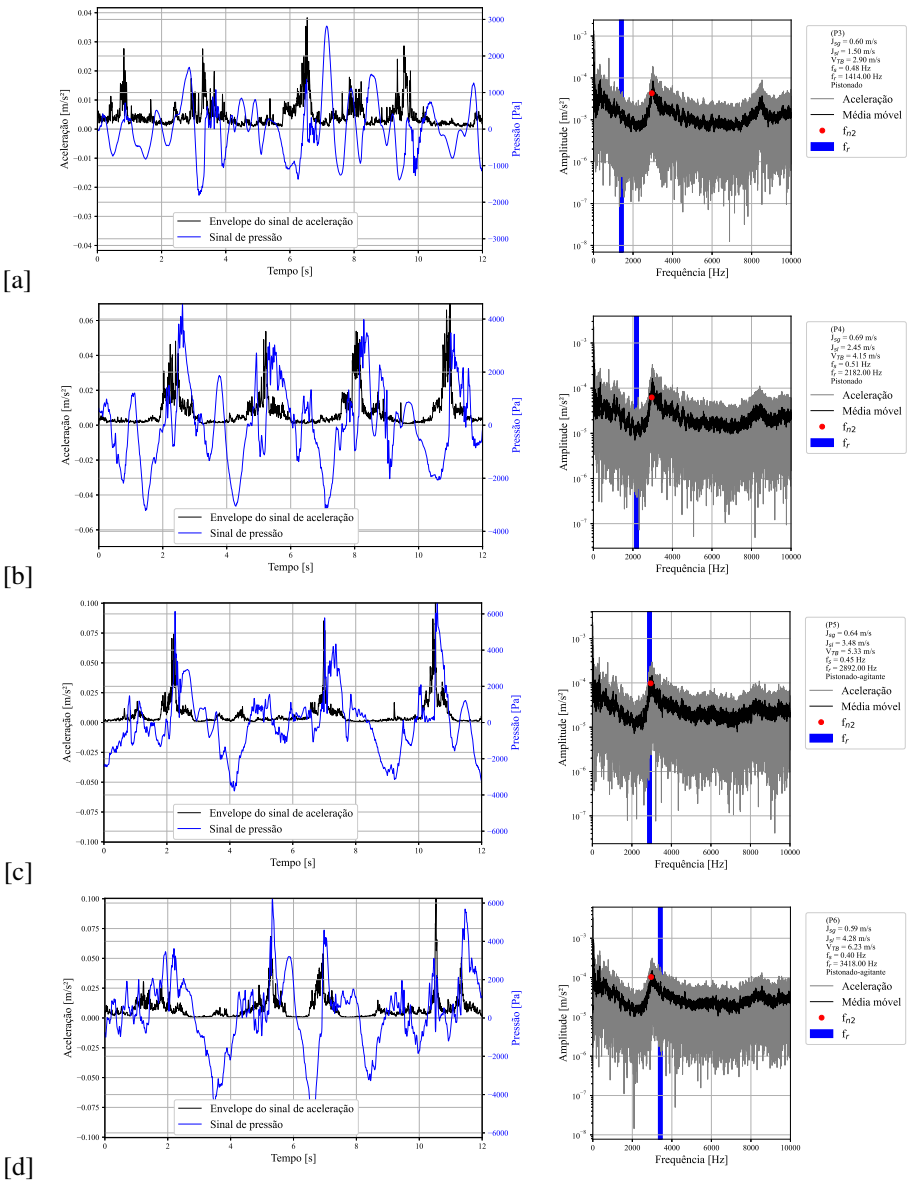

Figure 6 – Time series of pressure (red line) and acceleration signal envelope (black line) filtered, on the left. Acceleration signal DFT, cylindrical shell frequency $fn2$ (red dot) and resonance frequency f_r are indicated (blue line), on the right, for water-gas flow.

Petroleum (LabPetro) 'Kelsen Valente Serra', at the Center for Petroleum Studies (CEPETRO), University of Campinas for the experimental facilities.

REFERENCES

BARNEA, D. et al., 1980, "Flow pattern transition for gas-liquid flow in horizontal and inclined pipes. Comparison of experimental data with theory", International Journal of Multiphase Flow, v. 6, n. 3, pp. 217–225.

BARNEA, D.; BRAUNER, N., 1985, "Holdup of the liquid slug in two phase intermittent flow", International Journal of Multiphase Flow, v. 11, n. 1, p. 43–49.

BRENNEN, C. E. 2005,"Fundamentals of multiphase flow". [S.l.: s.n.], . v. 53. 1689–1699 p. ISSN 1098-6596. ISBN 9788578110796.

CARVALHO, F. et al., 2019, "Flow pattern classification in liquid-gas flows using flow-induced vibration", Experimental Thermal and Fluid Science, Elsevier Inc., v. 112, pp. 109950.

CALDERBANK, P., 1958, "Physical Rate Processes in Industrial Fermentation", Part I: The Interfacial Area in Gas–Liquid Contacting with MechanicalAgitation. Trans. Inst. Chem., v. 36, p. 443–463.

FAHY, F.; GARDONIO, P., 2015, "Sound and Structural Vibration Radiation, Transmission and Response". Academic Press in an imprint of Elsevier. pp 1–27.

FULLER, C. R.; FAHY, F. J., 1982, "And energy shells in cylindrical with", Journal of Sound and Vibration, v. 81, n. 4, pp. 501–518.

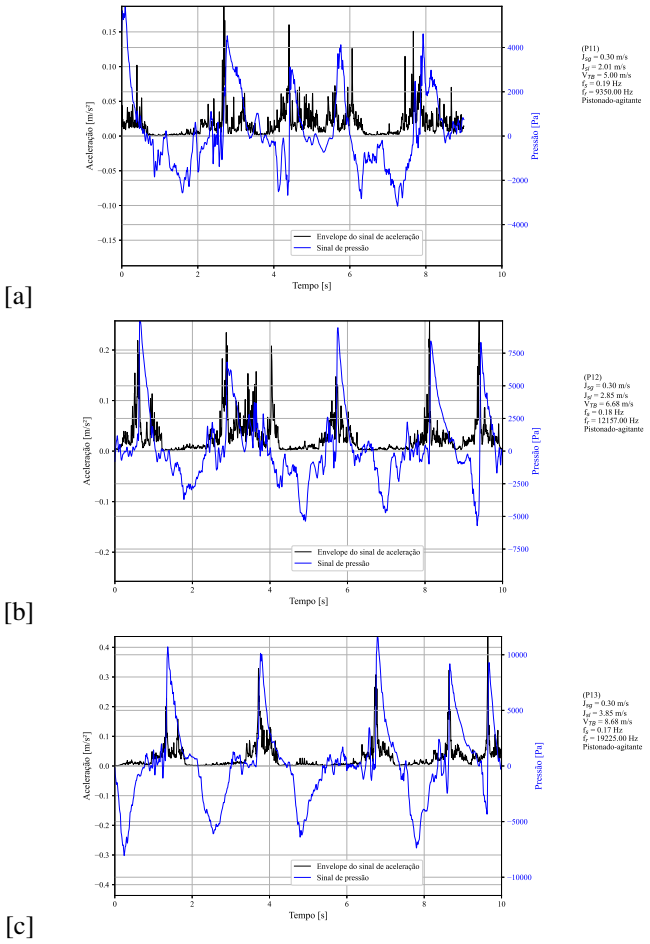

[a]

[b]

[c]

Figure 7 – Time series of pressure (blue line) and acceleration signal envelope (black line) filtered for oil-air flow.

HARA, F., 1977, ”Two-Phase-Flow-Induced Vibrations in a Horizontal Pulping System”, Bulletin of JSME, n. 43, pp. 463–470.

HINZE, J. O.,1955, ”Fundamentals of the hydrodynamic mechanism of splitting in dispersion processes”. AIChE Journal, v. 1, n. 3, p. 289–295.

ISHII, M.; HIBIKI, T., 2011, ”Thermo-fluid dynamics of two-phase flow”, pp 1–66.

MIWA, S. et al., 2015, ”Two-phase flow induced vibration in piping systems”, Progress in Nuclear Energy, Elsevier Ltd, v. 78, n. 2015, pp. 270–284.

MOHMMED, A. O. et al., 2020, ”One-way coupled fluid–structure interaction of gas–liquid slug flow in a horizontal pipe: Experiments and simulations”, Journal of Fluids and Structures, Elsevier Inc., v. 97, pp. 103083.

NORTON, M. P.; BULL, M. K., 1984, ”Mechanisms of the generation of external a acoustic radiation from pipes due to internal flow disturbances”, Journal of Sound and Vibration, v. 94, pp. 105–146.

SHOHAM, O., 2006, ”Mechanistic modeling of gas-liquid two-phase flow in pipes”.

KIRBY, R.; DUAN, W., 2019, ”Guided wave propagation in cylindrical ducts with elastic walls enclosing a fluid moving with a uniform velocity”, Wave Motion, pp. 1–9.

LIAO, Y.; LUCAS, D., 2009, ”A literature review of theoretical models for drop and bubble breakup in turbulent dispersions”. Chemical Engineering Science, v. 64, n. 15, p. 3389–3406. ISSN 00092509.

ZHAO, W. et al. 2021, ”Bubble characteristics and turbulent dissipation rate in horizontal bubbly pipe flow”, AIP Advances, AIP Publishing, LLC, v. 11, n. 2. ISSN 21583226.

RESPONSIBILITY NOTICE

The author(s) is (are) the only responsible for the printed material included in this paper.